Johns Hopkins Engineering

Applied Machine Learning for Mechanical Engineers

Machine Learning of Dislocation-Induced Stress Fields and Interaction Forces, Part 1, B

Johns Hopkins
Whiting School of Engineering

Rafiei et al. (2020)

- By the end of this lecture, you will be able to:

  - Describe the research goal in Rafiei et al. (2020)
  - Describe the problems and constraints in Rafiei et al. (2020)
  - Describe the dislocation formulations in Rafiei et al. (2020)
  - Describe the machine learning models in Rafiei et al. (2020)
  - Describing the unbiased/enriched machine learning repository in Rafiei et al. (2020)

Rafiei, M. H., Gu, Y., & El-Awady, J. A. (2020). Machine Learning of Dislocation-Induced Stress Fields and Interaction Forces. JOM, 1-13.

Rafiei et al. (2020)

- Research Goals:
  - Goal 1: Machine learning the stress field induced by dislocation i, termed hereafter as the dislocation stress field problem,
  - Goal 2: Machine learning the glide component of the Peach-Koehler force induced by dislocation i onto dislocation j, termed hereafter the Peach-Koehler force problem.

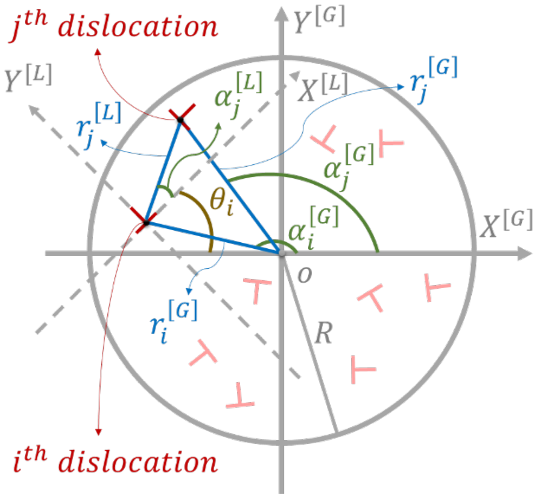

Focus is on approximation rather than an acceleration in 2D simulations

Rafiei, M. H., Gu, Y., & El-Awady, J. A. (2020). Machine Learning of Dislocation-Induced Stress Fields and Interaction Forces. JOM, 1-13.

Rafiei et al. (2020)

- Problems and Constraints:
  - The figure shows schematically a two-dimensional (2D) circular region of an infinite domain having radius R and containing randomly oriented and positioned infinite long edge dislocations. The origin of the global Cartesian coordinate system is at the center of the circular region and the X- and Y-axes are designated as $X^{[\mathrm{G}]}$ and $Y^{[\mathrm{G}]}$, respectively.
  - A local coordinate system is also defined at any dislocation "i" with its origin located at the dislocation position. The local X- and Y-axes are designated as $X^{[\mathrm{L}_i]}$ (direction of dislocation i's Burgers vector) and $Y^{[\mathrm{L}_i]}$ (direction of dislocation i's extra half-plane), respectively.
  - The Burgers vector in the global coordinate system of dislocation i is thus defined as: $\boldsymbol{B}_i = b[\cos(\theta_i), \sin(\theta_i), 0]$, where b is the Burgers vector magnitude (assumed constant for all dislocations) and $0 \leq \theta_i \leq 2\pi$ is the angle from $X^{[\mathrm{G}]}$ to $X^{[\mathrm{L}_i]}$.

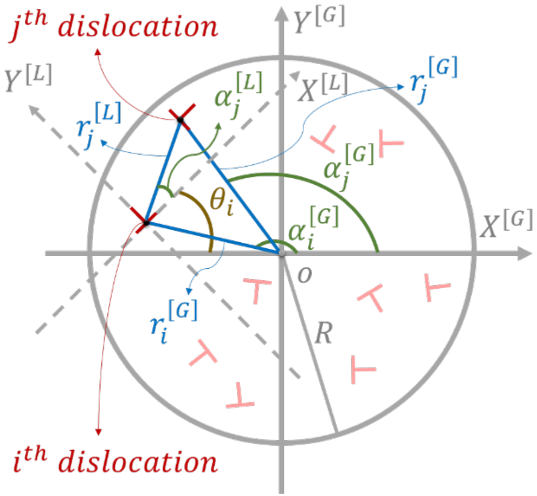

Rafiei, M. H., Gu, Y., & El-Awady, J. A. (2020). Machine Learning of Dislocation-Induced Stress Fields and Interaction Forces. JOM, 1-13.

Rafiei et al. (2020)

- Problems and Constraints:

  - The coordinates of any point in space can be described in any of the coordinate systems using the polar angle (i.e., azimuths), α, and the radial coordinate, r, where:

$$\begin{gathered} 0 \leq \alpha \leq 2\pi \\ 0 \leq r \leq R \end{gathered} \quad (1)$$

  - The position of dislocation i in the global coordinate system is designated by $\left(\alpha_i^{[G]}, r_i^{[G]}\right)$, while the coordinates of any point j in the local coordinate system of dislocation i is $\left(\alpha_j^{[L_i]}, r_j^{[L_i]}\right)$

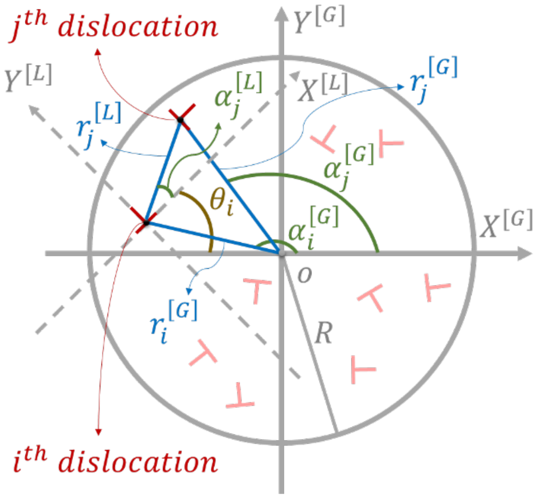

Rafiei, M. H., Gu, Y., & El-Awady, J. A. (2020). Machine Learning of Dislocation-Induced Stress Fields and Interaction Forces. JOM, 1-13.

Rafiei et al. (2020)

- Dislocation Formulations:

  - The stress field induced by dislocation i at point j in the local coordinate system of dislocation i can be expressed as follows

$$
\begin{aligned}
\sigma_{XX}^{[\mathrm{L}_i]} &= -\gamma \frac{3\sin\left(\alpha_j^{[\mathrm{L}_i]}\right) - 2\sin^3\left(\alpha_j^{[\mathrm{L}_i]}\right)}{r_j^{[\mathrm{L}_i]}} \\
\sigma_{YY}^{[\mathrm{L}_i]} &= \gamma \frac{\sin\left(\alpha_j^{[\mathrm{L}_i]}\right) - 2\sin^3\left(\alpha_j^{[\mathrm{L}_i]}\right)}{r_j^{[\mathrm{L}_i]}} \\
\sigma_{XY}^{[\mathrm{L}_i]} &= -\gamma \frac{\cos\left(\alpha_j^{[\mathrm{L}_i]}\right) - 2\cos^3\left(\alpha_j^{[\mathrm{L}_i]}\right)}{r_j^{[\mathrm{L}_i]}} \\
\sigma_{ZZ}^{[\mathrm{L}_i]} &= \nu\left(\sigma_{XX}^{[\mathrm{L}_i]} + \sigma_{YY}^{[\mathrm{L}_i]}\right) \\
\sigma_{XZ}^{[\mathrm{L}_i]} &= \sigma_{YZ}^{[\mathrm{L}_i]} = 0
\end{aligned}
\qquad (2)
$$

where $\gamma = Gb/2\pi(1-\nu)$, G is the shear modulus, and ν is the Poisson's ratio.

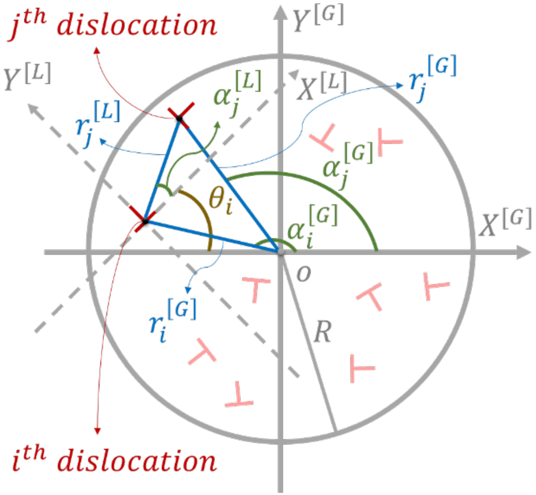

Rafiei, M. H., Gu, Y., & El-Awady, J. A. (2020). Machine Learning of Dislocation-Induced Stress Fields and Interaction Forces. JOM, 1-13.

Rafiei et al. (2020)

- Dislocation Formulations:
  - With respect to the global coordinate system, the stress field is:

$$
\begin{aligned}
\sigma_{XX}^{[G]} &= \sigma_{XX}^{[L_i]} \cos^2(\theta_i) + \sigma_{YY}^{[L_i]} - 2\sigma_{XY}^{[L_i]} \sin(\theta_i)\cos(\theta_i) \\
\sigma_{YY}^{[G]} &= \sigma_{XX}^{[L_i]} \sin^2(\theta_i) + \sigma_{YY}^{[L_i]} \cos^2(\theta_i) + 2\,\sigma_{XY}^{[L_i]} \sin(\theta_i)\cos(\theta_i) \\
\sigma_{XY}^{[G]} &= -\left[\sigma_{YY}^{[L_i]} - \sigma_{XX}^{[L_i]}\right] \sin(\theta_i)\cos(\theta_i) + \sigma_{XY}^{[L_i]} \left[\cos^2(\theta_i) - \sin^2(\theta_i)\right] \\
\sigma_{ZZ}^{[G]} &= \nu\left(\sigma_{XX}^{[G]} + \sigma_{YY}^{[G]}\right) \\
\sigma_{XZ}^{[G]} &= \sigma_{YZ}^{[G]} = 0
\end{aligned}
\tag{3}
$$

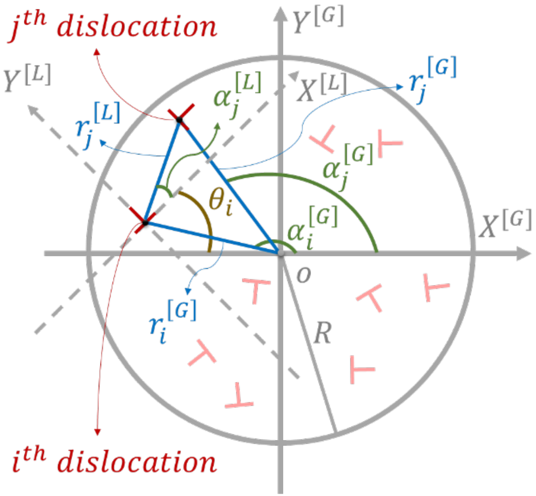

Rafiei, M. H., Gu, Y., & El-Awady, J. A. (2020). Machine Learning of Dislocation-Induced Stress Fields and Interaction Forces. JOM, 1-13.

Rafiei et al. (2020)

- Dislocation Formulations:
  - Simplified version:

$$\begin{aligned}
\sigma_{XX}^{[\mathrm{G}]} &= -\left(\gamma/2r_j^{[\mathrm{L}_i]}\right)\left[\sin\left(\alpha_j^{[\mathrm{L}_i]}+2\theta_i\right)+\sin\left(3\alpha_j^{[\mathrm{L}_i]}+2\theta_i\right)+2\sin\left(\alpha_j^{[\mathrm{L}_i]}\right)\right]\\
\sigma_{YY}^{[\mathrm{G}]} &= \left(\gamma/2r_j^{[\mathrm{L}_i]}\right)\left[\sin\left(\alpha_j^{[\mathrm{L}_i]}+2\theta_i\right)+\sin\left(3\alpha_j^{[\mathrm{L}_i]}+2\theta_i\right)-2\sin\left(\alpha_j^{[\mathrm{L}_i]}\right)\right]\\
\sigma_{XY}^{[\mathrm{G}]} &= \left(\gamma/2r_j^{[\mathrm{L}_i]}\right)\left[\cos\left(3\alpha_j^{[\mathrm{L}_i]}+2\theta_i\right)+\cos\left(\alpha_j^{[\mathrm{L}_i]}+2\theta_i\right)\right]\\
\sigma_{ZZ}^{[\mathrm{G}]} &= \nu\left(\sigma_{XX}^{[\mathrm{G}]}+\sigma_{YY}^{[\mathrm{G}]}\right)\\
\sigma_{XZ}^{[\mathrm{G}]} &= \sigma_{YZ}^{[\mathrm{G}]} = 0
\end{aligned} \tag{4}$$

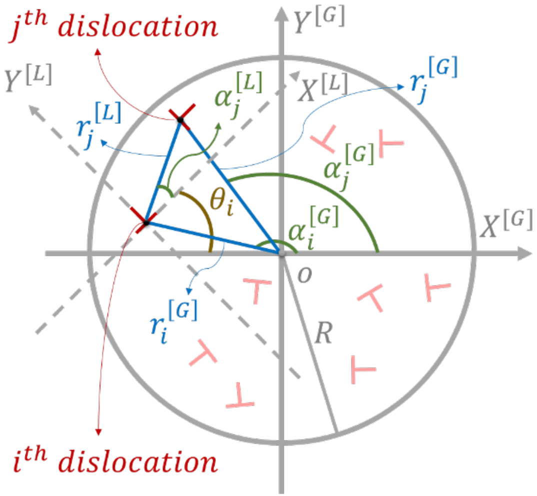

Rafiei, M. H., Gu, Y., & El-Awady, J. A. (2020). Machine Learning of Dislocation-Induced Stress Fields and Interaction Forces. JOM, 1-13.

Rafiei et al. (2020)

- Dislocation Formulations:

  - Peach-Koehler force:

$$\boldsymbol{F}^{ji} = \left(\boldsymbol{\sigma}^{[\mathrm{G}]} \cdot \boldsymbol{B}_j\right) \times \boldsymbol{\xi}$$

Where $\boldsymbol{\sigma}^{[\mathrm{G}]}$ is the stress tensor having components defined by Eq. (4), $\boldsymbol{B}_j = b\left[\cos\left(\theta_j\right), \sin\left(\theta_j\right), \ 0\right]$ is the Burgers vector of dislocation j, and $\boldsymbol{\xi} = (0, 0, 1)$ is the dislocation line direction

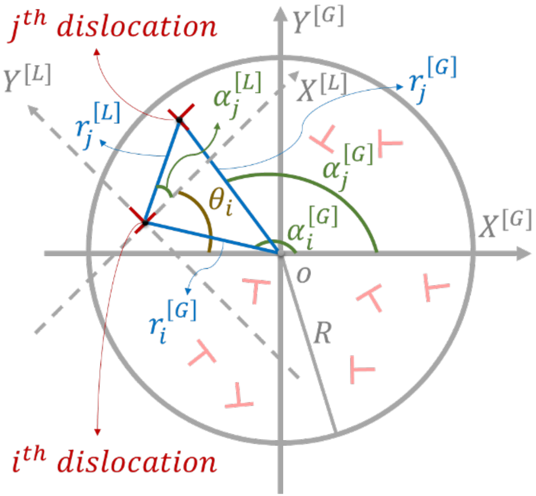

Rafiei, M. H., Gu, Y., & El-Awady, J. A. (2020). Machine Learning of Dislocation-Induced Stress Fields and Interaction Forces. JOM, 1-13.

Rafiei et al. (2020)

- Dislocation Formulations:
  - The glide component of this Peach-Koehler force:

$$f_{\mathrm{glide}}^{ji} = \left[\left(\boldsymbol{\sigma}^{[\mathrm{G}]} \cdot \boldsymbol{B}_j\right) \times \boldsymbol{\xi}\right] \cdot \frac{\boldsymbol{B}_j}{b}$$
$$= \left(\gamma b / 2 r_j^{[\mathrm{L}_i]}\right)\left[\cos\left(3\alpha_j^{[L_i]} - 2\theta_j + 2\theta_i\right) + \cos\left(\alpha_j^{[L_i]} - 2\theta_j + 2\theta_i\right)\right] \quad (5)$$

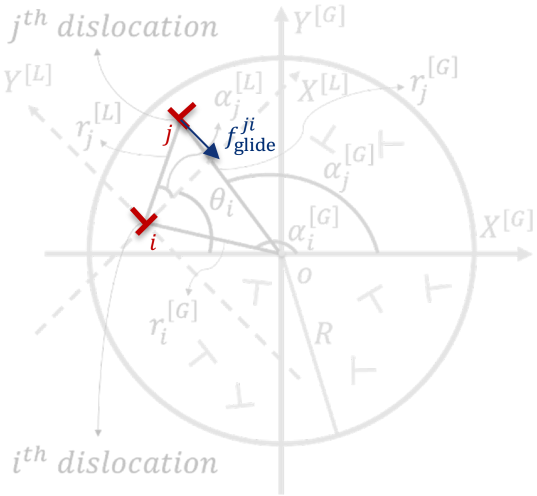

Rafiei, M. H., Gu, Y., & El-Awady, J. A. (2020). Machine Learning of Dislocation-Induced Stress Fields and Interaction Forces. JOM, 1-13.

Rafiei et al. (2020)

- Dislocation Formulations:
  - In DDD simulations a critical distance of $d \sim 3b$ is typically defined between any two dislocations for practical and computational efficiency.
  - Below this critical distance, the repulsive (or attractive) forces between both dislocations will be so high that they will be driven far away from one another (or collide with each other) within a fraction of the simulation time step, which is typically on the order of 10^{-11} s.
  - Thus, the current analysis will be confined to cases were point j is at a distance $d \geq 3b$ from dislocation i. Therefore, the constraint for the distance between any two dislocations is:

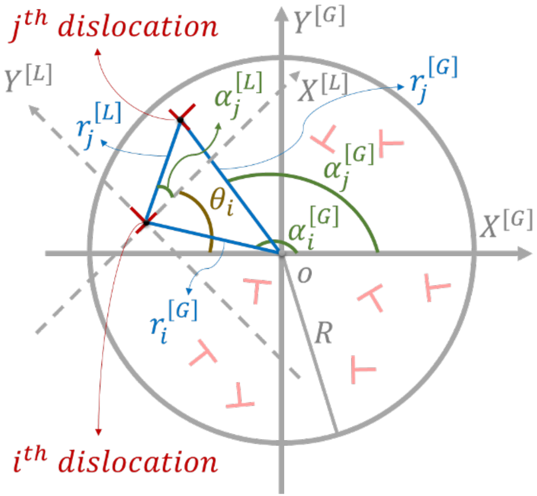

$$d \leq \sqrt{\left[r_i^{[G]} \sin\left(\alpha_i^{[G]}\right) - r_j^{[G]} \sin\left(\alpha_j^{[G]}\right)\right]^2 + \left[r_i^{[G]} \cos\left(\alpha_i^{[G]}\right) - r_j^{[G]} \cos\left(\alpha_j^{[G]}\right)\right]^2} \quad (6)$$

Rafiei, M. H., Gu, Y., & El-Awady, J. A. (2020). Machine Learning of Dislocation-Induced Stress Fields and Interaction Forces. JOM, 1-13.

Rafiei et al. (2020)

(6)

- Machine Learning Models:
    - Universal approximation theorem suggests that multi-parameter continuous functions can be approximated by some ML techniques, here, we investigate the plausibility of using ML to estimate the dislocation stress fields.
    - ML model utilized here includes a deep neural network that has V input neurons, U outputs, and five dense hidden layers, each having 100, 75, 50, 25, and 12 neurons, respectively.
    - There is no need for any convolution, max- or average-pooling labels, or temporal-based layers such as long-short-term memory layers because there is neither image/multi-channel inputs sensitive to image positional/torsional attributes nor temporal-type data to use the output of the previous datapoint in the current input.
    - The learning algorithm is adaptive moment estimation, referred to as ADAM
    - For hidden layers, the activation function is rectified linear units, referred to as ReLu, and for the output layer, the activation function is selected to be linear.

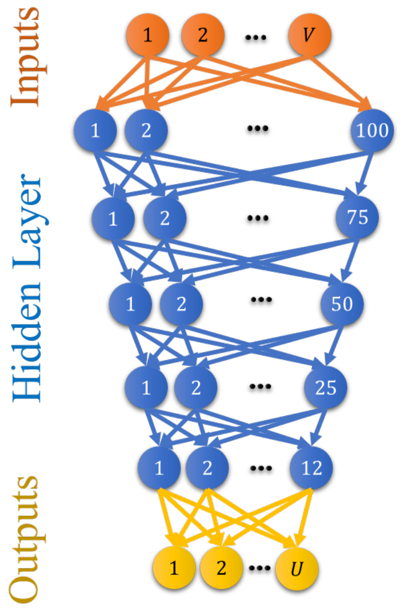

Rafiei, M. H., Gu, Y., & El-Awady, J. A. (2020). Machine Learning of Dislocation-Induced Stress Fields and Interaction Forces. JOM, 1-13.

Rafiei et al. (2020)

- Machine Learning Models:
  - Machine learning the dislocation-induced stress field
    - The stress field at point j due to dislocation i as defined by Eq. (4) can be determined given $\alpha_i^{[G]}$, $r_i^{[G]}$, θ_i, $\alpha_j^{[G]}$, and $r_j^{[G]}$. However, only the position of point j in the local coordinate system of i is unique, irrespective of the global position of i and j. Thus, the input vector to the ML model is uniquely defined by three inputs:

$$\boldsymbol{V} = \left[\alpha_j^{[L_i]}, \log\left(r_j^{[L_i]}\right), \theta_i\right] \qquad (7)$$

    - The output vector to be machine learned is the three dimensionless stress components:

$$\boldsymbol{U} = \left[\frac{\sigma_{XX}^{[G]}}{\gamma}, \frac{\sigma_{YY}^{[G]}}{\gamma}, \frac{\sigma_{XY}^{[G]}}{\gamma}\right] \qquad (8)$$

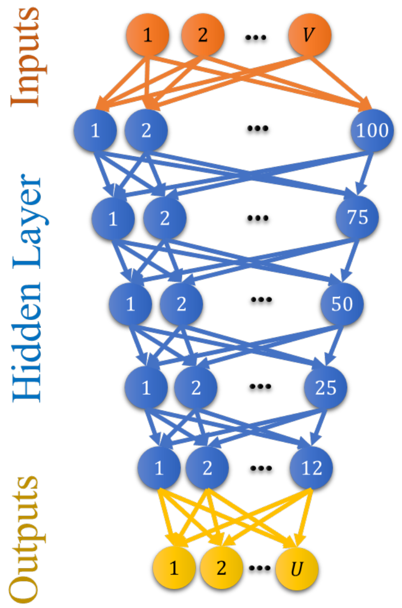

Rafiei, M. H., Gu, Y., & El-Awady, J. A. (2020). Machine Learning of Dislocation-Induced Stress Fields and Interaction Forces. JOM, 1-13.

Rafiei et al. (2020)

- Machine Learning Models:
  - Machine learning the glide component of the dislocation interactions induced Peach-Koehler force
    - The glide component of the Peach-Koehler force on dislocation j due to dislocation i as defined by Eq. (5) can be determined given $\alpha_i^{[G]}$, $r_i^{[G]}$, θ_i, $\alpha_j^{[G]}$, $r_j^{[G]}$, and θ_j. Similar to the ML of the dislocation stress field problem, only the relative position of dislocation j with respect to dislocation i is unique. Thus, the input vector to the ML model can be defined by four inputs

$$\boldsymbol{V} = \left[\alpha_j^{[\mathrm{L}_i]}, \log\left(r_j^{[\mathrm{L}_i]}\right), \theta_j, \theta_i\right] \qquad (9)$$

    - The output to be machine learned is the dimensionless glide component of the Peach-Koehler force:

$$\boldsymbol{U} = \left[\frac{f_{\mathrm{glide}}^{ji}}{\gamma b}\right] \qquad (10)$$

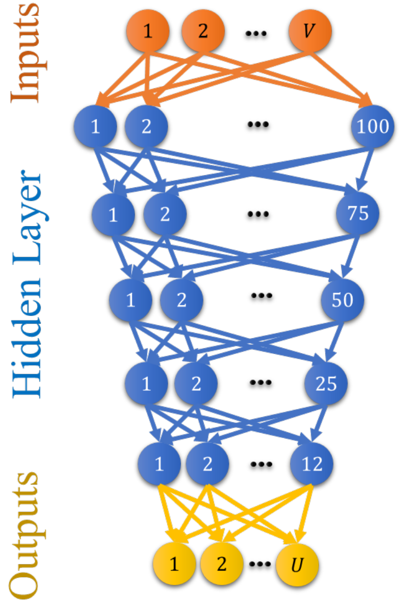

Rafiei, M. H., Gu, Y., & El-Awady, J. A. (2020). Machine Learning of Dislocation-Induced Stress Fields and Interaction Forces. JOM, 1-13.

Rafiei et al. (2020)

- Unbiased/Enriched Machine Learning Repository:
  - Machine learning models require generating representative training datasets (i.e., input and output datasets). Biased ML models are usually the unintended consequence of biased training data repository
  - In fact, in both regression and classification problems, a perfect enriched repository, also referred to as balanced repository, is group-independent and covers ample samples with uniformly distributed attributes that are limited between pre-defined constraints
  - For the current study, one might generate uniformly distributed random dislocation coordinates and/or Burgers vectors in space as the ML inputs (i.e., Eq. (7) or (9)) and compute the corresponding outputs (i.e., Eq. (8) or (10)) to serve as the repository for training a regression ML model.
  - Although the input distribution will be uniform, the outputs, whether stresses or Peach-Koehler forces, will be poorly distributed since both are inversely proportional to $r_j^{[L]}$ (i.e., the frequency of near-zero values is significantly higher than all other possible values).

Rafiei, M. H., Gu, Y., & El-Awady, J. A. (2020). Machine Learning of Dislocation-Induced Stress Fields and Interaction Forces. JOM, 1-13.

Rafiei et al. (2020)

- Unbiased/Enriched Machine Learning Repository:
  - Figure (top left) represents 10,000 uniformly distributed random coordinates in the simulation cell for dislocations i and j.
  - Dislocation coordinates and the Burgers vector angles are uniformly generated (top right plots).
  - However, magnitudes of $\sigma_{XX}^{[G]}/\gamma$, $\sigma_{YY}^{[G]}/\gamma$, $\sigma_{XY}^{[G]}/\gamma$, and $f_{\text{glide}}^{ji}/\gamma b$, are all poorly distributed (bottom plots) and predominantly near-zero.

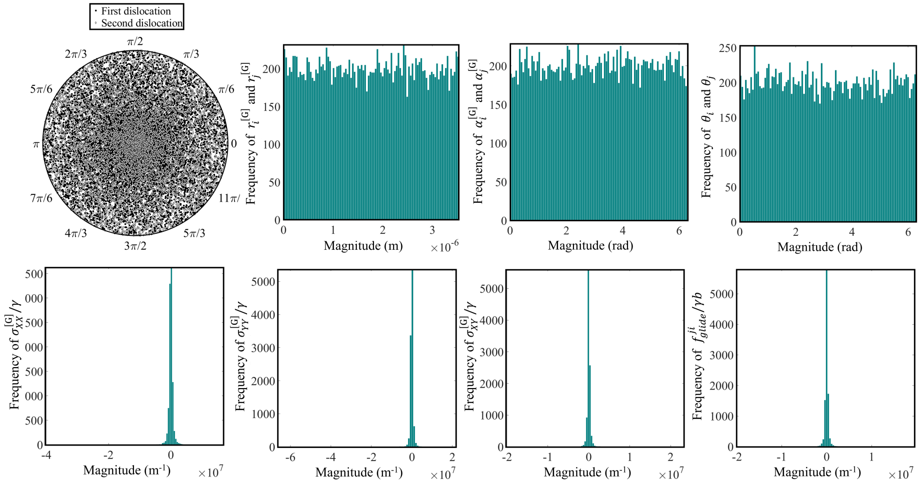

Rafiei, M. H., Gu, Y., & El-Awady, J. A. (2020). Machine Learning of Dislocation-Induced Stress Fields and Interaction Forces. JOM, 1-13.

Rafiei et al. (2020)

- Unbiased/Enriched Machine Learning Repository:
  - This is due to that the stress field, and accordingly, the Peach-Koehler force magnitude, are inversely proportional to the distance between i and j.
  - This is an example of biased distribution of an output dataset, even though the inputs are uniformly distributed.
  - By employing such a repository, a typical ML model will tend to learn the patterns of near-zero values as compared to larger values.
  - ML models trained by such biased repositories will generally produce poor predictions.

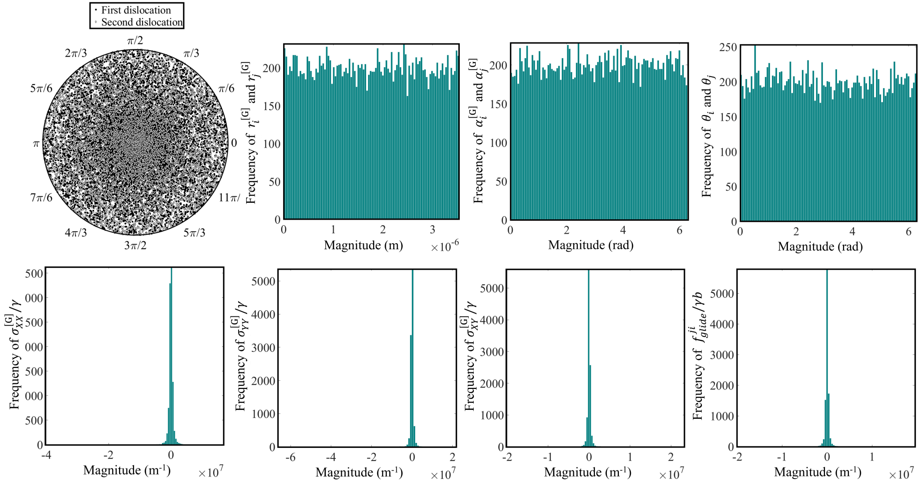

Rafiei, M. H., Gu, Y., & El-Awady, J. A. (2020). Machine Learning of Dislocation-Induced Stress Fields and Interaction Forces. JOM, 1-13.

Rafiei et al. (2020)

- Unbiased/Enriched Machine Learning Repository:
  - Enriched datasets are required such that they fairly represent the attribute space with respect to the problems' constraints
  - An appropriate repository includes relatively uniform distribution for both inputs and outputs.
  - To generate enriched repositories for the current problem, the outputs are "reverse engineered" to be uniform.
  - This is achieved by first generating uniform distributions of the stresses (i.e., $\sigma_{XX}^{[G]}/\gamma$, $\sigma_{YY}^{[G]}/\gamma$, and $\sigma_{XY}^{[G]}/\gamma$) for the stress field ML problem and the glide component of the Peach-Kohler force (i.e., f_{glide}^{ji}) for the Peach-Koehler force ML problem between the minimum and maximum feasible values using a uniform random distribution generator (URG).
  - Next, using the inverse of Eq. (4) for the stresses or Eq. (5) for the Peach-Koehler force, the corresponding inputs (e.g., polar coordinates and/or Burgers vector directions) can be calculated.

Rafiei, M. H., Gu, Y., & El-Awady, J. A. (2020). Machine Learning of Dislocation-Induced Stress Fields and Interaction Forces. JOM, 1-13.

Rafiei et al. (2020)

- Unbiased/Enriched Machine Learning Repository:
  - It should be noted that any continuous function has as many inverse functions as the number of its variables. Thus, for the stress field ML problem, the radial coordinates of j with respect to i can be computed as:

$$
\begin{aligned}
r_{j,XX}^{[\mathrm{L}_i]} &= -\left(\gamma/2\sigma_{XX}^{[\mathrm{G}]}\right)\left[\sin\left(\alpha_j^{[\mathrm{L}_i]}+2\theta_i\right)+\sin\left(3\alpha_j^{[\mathrm{L}_i]}+2\theta_i\right)+2\sin\left(\alpha_j^{[\mathrm{L}_i]}\right)\right] \\
r_{j,YY}^{[\mathrm{L}_i]} &= \left(\gamma/2\sigma_{YY}^{[\mathrm{G}]}\right)\left[\sin\left(\alpha_j^{[\mathrm{L}_i]}+2\theta_i\right)+\sin\left(3\alpha_j^{[\mathrm{L}_i]}+2\theta_i\right)-2\sin\left(\alpha_j^{[\mathrm{L}_i]}\right)\right] \\
r_{j,XY}^{[\mathrm{L}_i]} &= \left(\gamma/2\sigma_{XY}^{[\mathrm{G}]}\right)\left[\cos\left(3\alpha_j^{[\mathrm{L}_i]}+2\theta_i\right)+\cos\left(\alpha_j^{[\mathrm{L}_i]}+2\theta_i\right)\right]
\end{aligned}
\tag{11}
$$

where $r_{j,XX}^{[\mathrm{L}_i]}$, $r_{j,YY}^{[\mathrm{L}_i]}$, and $r_{j,XY}^{[\mathrm{L}_i]}$ are the radial coordinates that result in uniformly distributed $\sigma_{XX}^{[\mathrm{G}]}/\gamma$, $\sigma_{YY}^{[\mathrm{G}]}/\gamma$, and $\sigma_{XY}^{[\mathrm{G}]}/\gamma$, respectively.

Rafiei, M. H., Gu, Y., & El-Awady, J. A. (2020). Machine Learning of Dislocation-Induced Stress Fields and Interaction Forces. JOM, 1-13.

Rafiei et al. (2020)

- Unbiased/Enriched Machine Learning Repository:

  - For the glide component of the Peach-Kohler force problem, the radial coordinate of dislocation j with respect to i can be shown to be

$$r_{j,\text{glide}}^{[\mathrm{L}_i]} = \left(\frac{\gamma b}{f_{\text{glide}}^{ji}}\right)\left[\cos\left(3\alpha_j^{[L_i]} - 2\theta_j + 2\theta_i\right) + \cos\left(\alpha_j^{[L_i]} - 2\theta_j + 2\theta_i\right)\right] \qquad (12)$$

where $r_{j,\text{glide}}^{[\mathrm{L}_i]}$ is the radial coordinate that results in a uniformly distributed f_{glide}^{ji}

Rafiei, M. H., Gu, Y., & El-Awady, J. A. (2020). Machine Learning of Dislocation-Induced Stress Fields and Interaction Forces. JOM, 1-13.

Rafiei et al. (2020)

- Unbiased/Enriched Machine Learning Repository:

  - Other than $\sigma_{XX}^{[\mathrm{G}]}/\gamma$, $\sigma_{YY}^{[\mathrm{G}]}/\gamma$, $\sigma_{XY}^{[\mathrm{G}]}/\gamma$, and $f_{\mathrm{glide}}^{ji}/\gamma b$, all other parameters on the right-hand sides of Eqs. (11) and (12) are generated using a URG with respect to the aforementioned constraints.

  - For each $r_{j,XX}^{[\mathrm{L}_i]}$, $r_{j,YY}^{[\mathrm{L}_i]}$, and $r_{j,XY}^{[\mathrm{L}_i]}$ computed from Eq. (11), the corresponding stress field in Eq. (4) is then recomputed to generate the proper stress datapoint.

Rafiei, M. H., Gu, Y., & El-Awady, J. A. (2020). Machine Learning of Dislocation-Induced Stress Fields and Interaction Forces. JOM, 1-13.

Rafiei et al. (2020)

- Unbiased/Enriched Machine Learning Repository:
  - Example: 10^8 datapoints (i.e., inputs and outputs) have been generated for the stress problem.
  - Decreased to $\sim 3.6\times 10^7$ after enforcing the constraints of Eq. (1).
  - Histograms (i.e., magnitudes versus frequency) of $\alpha_j^{[\mathrm{L_i}]}$, $log\left(r_j^{[L_i]}\right)$, θ_i, $\sigma_{XX}^{[\mathrm{G}]}/\gamma$, $\sigma_{YY}^{[\mathrm{G}]}/\gamma$, and $\sigma_{XY}^{[\mathrm{G}]}/\gamma$ that correspond to these datapoints.
  - Histograms are not uniform since $\sim 6.4\times 10^7$ datapoints have been discarded from the repository due to constraint violations.
  - Nevertheless, the resulting histograms are considerably better (i.e., have a lower standard deviation of frequencies) than the corresponding histograms in the previous slides

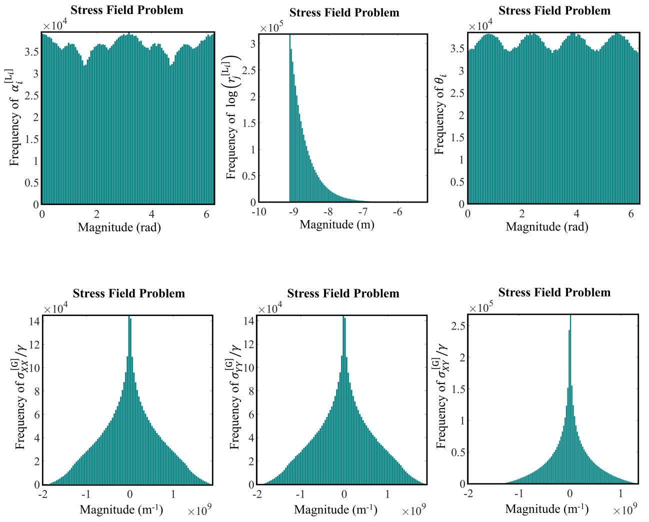

Rafiei, M. H., Gu, Y., & El-Awady, J. A. (2020). Machine Learning of Dislocation-Induced Stress Fields and Interaction Forces. JOM, 1-13.

Rafiei et al. (2020)

- Unbiased/Enriched Machine Learning Repository:
  - Example: 10^8 datapoints (i.e., inputs and outputs) have been generated for the Peach-Koehler problem.
  - Decreased to $\sim 4.1\times 10^7$ after enforcing the constraints of Eq. (1).
  - Histograms (i.e., magnitudes versus frequency) of $\alpha_j^{[\mathrm{L_i}]}$, $log\left(r_j^{[L_i]}\right)$, θ_i, $\sigma_{XX}^{[\mathrm{G}]}/\gamma$, $\sigma_{YY}^{[\mathrm{G}]}/\gamma$, and $\sigma_{XY}^{[\mathrm{G}]}/\gamma$ that correspond to these datapoints.
  - Histograms are not uniform since $\sim 5.9\times 10^7$ datapoints have been discarded from the repository due to constraint violations.
  - Nevertheless, the resulting histograms are considerably better (i.e., have a lower standard deviation of frequencies) than the corresponding histograms in the previous slides

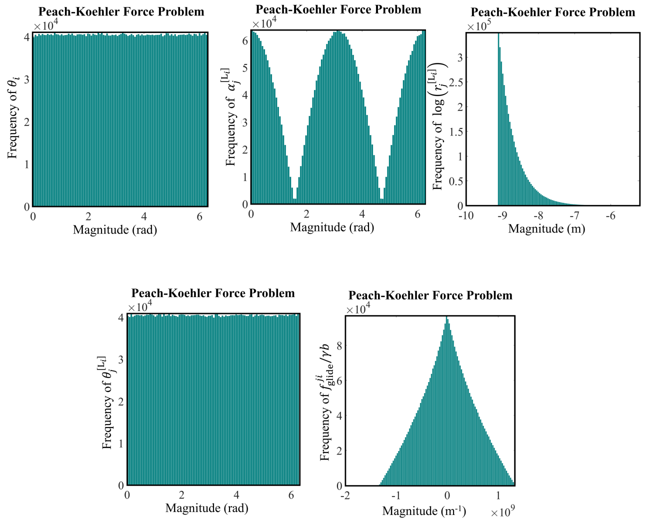

Rafiei, M. H., Gu, Y., & El-Awady, J. A. (2020). Machine Learning of Dislocation-Induced Stress Fields and Interaction Forces. JOM, 1-13.

Rafiei et al. (2020)

- In this lecture, you learned about:
  - The research goal in Rafiei et al. (2020)
  - The problems and constraints in Rafiei et al. (2020)
  - The dislocation formulations in Rafiei et al. (2020)
  - The machine learning models in Rafiei et al. (2020)
  - The unbiased/enriched machine learning repository in Rafiei et al. (2020)

- In the next Module, we will practice machine learning dislocation model of Rafiei et al., 2020 in Python.

Rafiei, M. H., Gu, Y., & El-Awady, J. A. (2020). Machine Learning of Dislocation-Induced Stress Fields and Interaction Forces. JOM, 1-13.

JOHNS HOPKINS

WHITING SCHOOL
of ENGINEERING